IOP Publishing and International Atomic Energy Agency Nuclear Fusion
Nucl. Fusion **52** (2012) 023005 (11pp) doi:10.1088/0029-5515/52/2/023005

Gyrokinetic simulation model for kinetic magnetohydrodynamic processes in magnetized plasmas

W. Deng[1], **Z. Lin**[1,2,a] **and I. Holod**[1]

[1] Department of Physics and Astronomy, University of California, Irvine, CA 92697, USA
[2] Fusion Simulation Center, Peking University, Beijing 100871, People's Republic of China

E-mail: zhihongl@uci.edu

Received 17 October 2011, accepted for publication 16 December 2011
Published 12 January 2012
Online at stacks.iop.org/NF/52/023005

Abstract
A nonlinear gyrokinetic simulation model incorporating equilibrium current has been formulated for studying kinetic magnetohydrodynamic processes in magnetized plasmas. This complete formulation enables gyrokinetic simulation of both pressure-gradient-driven and current-driven instabilities as well as their nonlinear interactions in multi-scale simulations. The gyrokinetic simulation model recovers the ideal magnetohydrodynamic theory in the linear long wavelength regime including ideal and kinetic ballooning modes, kink modes and shear Alfvén waves. The implementation of this model in the global gyrokinetic particle code has been verified for the simulation of the effects of equilibrium current on the reversed shear Alfvén eigenmode in tokamaks.

1. Introduction

Gyrokinetic simulation is useful for studying drift wave instabilities and kinetic magnetohydrodynamic (MHD) modes, such as interchange modes, kink modes and shear Alfvén waves excited by energetic particles, where kinetic effects are important. With a recent electromagnetic upgrade [1], the global gyrokinetic toroidal code (GTC) [2] has been successfully applied to the simulations of various Alfvén eigenmodes in tokamaks including toroidal Alfvén eigenmodes (TAEs) [3], reversed shear Alfvén eigenmodes (RSAEs) [4] and beta-induced Alfvén eigenmodes (BAEs) [5]. Previous gyrokinetic simulations treat only pressure-driven instabilities. In this work we further extend the formulation of the gyrokinetic simulation model in GTC to include equilibrium current, which affects the existence condition of RSAE [4, 6] and excites current-driven modes such as the kink mode [7]. Nonlinear electron effects are also added in the electron continuity equation [1], which enables fully nonlinear electromagnetic simulations. In the linear and long wavelength limit, this gyrokinetic formulation is shown to reduce to the ideal MHD theory. The implementation of the equilibrium current is verified in RSAE simulations by comparing with the analytic theory.

This paper first presents the nonlinear gyrokinetic formulation with equilibrium current in section 2. Then the formulation in the linear long wavelength limit is shown to reduce to the ideal MHD theory in section 3. The verification of the implementation of the equilibrium current in RSAE simulations is shown in section 4. The conclusions are given in section 5.

2. Nonlinear gyrokinetic formulation with equilibrium current

In this gyrokinetic formulation used in GTC, the ions are described by the gyrokinetic equation [8]. Although GTC can do both δf and full-f simulations, in this work only δf simulation is considered. With quantities decomposed into equilibrium and perturbed components, and the parallel perturbed magnetic field $\delta \boldsymbol{B}_\parallel$ ignored for low-β plasmas, the gyrokinetic equation reads

$$(\partial_t + \dot{\boldsymbol{X}} \cdot \nabla + \dot{v}_\parallel \partial_{v_\parallel})[f_0(\boldsymbol{X}, \mu, v_\parallel) + \delta f(\boldsymbol{X}, \mu, v_\parallel, t)] = 0, \tag{1}$$

$$\dot{\boldsymbol{X}} = v_\parallel \frac{\boldsymbol{B}_0 + \langle \delta \boldsymbol{B} \rangle_c}{B_0} + \underbrace{\frac{c\boldsymbol{b}_0 \times \nabla \langle \phi \rangle_c}{B_0}}_{\langle \boldsymbol{v}_E \rangle_c} + \underbrace{\frac{v_\parallel^2}{\Omega} \nabla \times \boldsymbol{b}_0}_{\boldsymbol{v}_c} + \underbrace{\frac{\mu}{m\Omega} \boldsymbol{b}_0 \times \nabla B_0}_{\boldsymbol{v}_g}, \tag{2}$$

[a] Author to whom any correspondence should be addressed.

$$\dot{v}_\parallel = -\frac{1}{m}\frac{\boldsymbol{B}_0 + \frac{B_0 v_\parallel}{\Omega}\nabla\times\boldsymbol{b}_0 + \langle\delta\boldsymbol{B}\rangle_c}{B_0}\cdot(\mu\nabla B_0 + Z\nabla\langle\phi\rangle_c) - \frac{Z}{mc}\partial_t\langle A_\parallel\rangle_c, \tag{3}$$

where f_0 and δf denote the equilibrium and the perturbed distribution function, respectively; $\boldsymbol{X}$, $v_\parallel$, μ, m, Z and Ω denote the gyro-centre position, the parallel velocity, the magnetic moment, the mass, the electric charge and the cyclotron angular frequency, respectively; $\boldsymbol{B}_0$, $\delta\boldsymbol{B}$, ϕ and $A_\parallel$ denote the equilibrium and the perturbed magnetic field, the electrostatic potential and the parallel vector potential, respectively; $\boldsymbol{b}_0 \equiv \boldsymbol{B}_0/B_0$; $\boldsymbol{v}_E$, $\boldsymbol{v}_c$ and $\boldsymbol{v}_g$ denote the $\boldsymbol{E}\times\boldsymbol{B}$ drift velocity, the curvature drift velocity and the grad-B drift velocity, respectively; c and t denote the light speed and the time, respectively;

$$\langle\cdot\rangle_c \equiv \int \frac{d\vartheta_c}{2\pi} d\boldsymbol{x}\,\delta(\boldsymbol{X}+\boldsymbol{\rho}-\boldsymbol{x}) \tag{4}$$

denotes gyro-averaging with ϑ_c, $\boldsymbol{x}$ and $\boldsymbol{\rho}$ being the gyro-phase angle, the particle position and the gyro-radius vector. Here zero equilibrium electric field ($\phi_0 = 0$) and time-independent equilibrium magnetic field ($\partial_t A_{\parallel 0} = 0$) are assumed, so ϕ and $A_\parallel$ are used to denote the perturbed potentials including the zonal and nonzonal components:

$$\phi = \phi_{00} + \delta\phi, \qquad A_\parallel = A_{\parallel 00} + \delta A_\parallel, \tag{5}$$

where ϕ_{00} and $A_{\parallel 00}$ are zonal components, and $\delta\phi$ and $\delta A_\parallel$ are nonzonal components.

The electromagnetic field is described by the gyrokinetic Poisson equation [9] and Ampère's law [1]:

$$\frac{Z_i^2 n_i}{T_i}(\phi - \tilde{\phi}) = \sum_{\alpha=i,e} Z_\alpha\,\delta n_\alpha, \tag{6}$$

$$-\frac{c}{4\pi}\nabla_\perp^2 A_\parallel = \sum_{\alpha=i,e}\delta J_{\parallel\alpha}, \tag{7}$$

where for the ion species [10],

$$\delta\tilde{\phi}(\boldsymbol{x},t) = \frac{1}{n_i}\int_{\boldsymbol{X}\to\boldsymbol{x}} d\boldsymbol{v}\, f_i(\boldsymbol{X},\mu,v_\parallel,t)\langle\delta\phi\rangle_c(\boldsymbol{X},t), \tag{8}$$

$$\delta n_i(\boldsymbol{x},t) = \int_{\boldsymbol{X}\to\boldsymbol{x}} d\boldsymbol{v}\,\delta f_i(\boldsymbol{X},\mu,v_\parallel,t), \tag{9}$$

$$\delta J_{\parallel i}(\boldsymbol{x},t) = \int_{\boldsymbol{X}\to\boldsymbol{x}} d\boldsymbol{v} Z_i v_\parallel\,\delta f_i(\boldsymbol{X},\mu,v_\parallel,t). \tag{10}$$

Here the integral symbol represents the integral over the gyro-centre velocity space and the transformation between the gyro-centre and the particle coordinates:

$$\int_{\boldsymbol{X}\to\boldsymbol{x}} d\boldsymbol{v} \equiv \int \frac{2\pi B_0}{m} d\mu\, dv_\parallel \int \frac{d\vartheta_c}{2\pi} d\boldsymbol{X}\,\delta(\boldsymbol{X}+\boldsymbol{\rho}-\boldsymbol{x}). \tag{11}$$

For electrons, the particle position and the gyro-centre position are not distinguished because of their small gyro-radii ($k_\perp\rho_e \ll 1$, where $k_\perp = |\nabla_\perp|$) in the drift-kinetic limit, so their density and current are simply just ($Z_e = -e$):

$$\delta n_e = \int_{GC} d\boldsymbol{v}\,\delta f_e, \tag{12}$$

$$\delta J_{\parallel e} = -e\int_{GC} d\boldsymbol{v} v_\parallel\,\delta f_e, \tag{13}$$

where

$$\int_{GC} d\boldsymbol{v} \equiv \int \frac{2\pi B_0}{m} d\mu\, dv_\parallel. \tag{14}$$

To obtain good numerical properties in ion scale simulations, the electrons are simulated using a fluid-kinetic hybrid model [1, 11] in GTC. In section 2.1, the electron continuity equation is extended to include the equilibrium current and nonlinear effects.

GTC solves the ion gyrokinetic equation and the kinetic part of the electron hybrid model using the particle-in-cell method. The perturbed distribution function is carried by the marker particle weight w. For ions, $w_i \equiv \delta f_i/f_i$. For electrons, $w_e \equiv \delta h_e/f_e$, where δh_e is the nonadiabatic part of the electron perturbed distribution function. In section 2.2, the weight evolution equations are extended to include the equilibrium current.

2.1. Electron continuity equation

Since electron's gyro-radius is much smaller than ion's, we take the drift-kinetic limit of (1) for electrons by removing the gyro-averaging operator $\langle\cdot\rangle_c$. Integrating (1) in the drift-kinetic limit over the guiding centre velocity space $\int_{GC} d\boldsymbol{v}$, we get an equilibrium equation and a perturbed equation. The equilibrium continuity equation writes:

$$\boldsymbol{B}_0\cdot\nabla\left(\frac{n_0 u_{\parallel 0}}{B_0}\right) + \frac{c\nabla\times\boldsymbol{b}_0}{Z}\cdot\nabla\left(\frac{P_{\parallel 0}}{B_0}\right) + \frac{c\boldsymbol{b}_0\times\nabla B_0}{Z}\cdot\nabla\left(\frac{P_{\perp 0}}{B_0^2}\right) + \frac{c\nabla\times\boldsymbol{b}_0\cdot\nabla B_0}{ZB_0^2}P_{\perp 0} = 0, \tag{15}$$

where

$$n_0 = \int_{GC} d\boldsymbol{v} f_0, \tag{16}$$

$$u_{\parallel 0} = \frac{1}{n_0}\int_{GC} d\boldsymbol{v} v_\parallel f_0, \tag{17}$$

$$P_{\parallel 0} = \int_{GC} d\boldsymbol{v} m v_\parallel^2 f_0, \tag{18}$$

$$P_{\perp 0} = \int_{GC} d\boldsymbol{v}\mu B_0 f_0. \tag{19}$$

The neoclassical equilibrium flow $u_{\parallel 0}$ in (15) is determined by the neoclassical theory [12]. The perturbed continuity equation is

$$\begin{aligned} 0 = {} & \partial_t\,\delta n + \delta\boldsymbol{B}\cdot\nabla\left(\frac{n_0 u_{\parallel 0}}{B_0}\right) + B_0\boldsymbol{v}_E\cdot\nabla\left(\frac{n_0}{B_0}\right) \\ & + \boldsymbol{B}_0\cdot\nabla\left(\frac{n_0\,\delta u_\parallel}{B_0}\right) + \frac{c\nabla\times\boldsymbol{b}_0}{Z}\cdot\nabla\left(\frac{\delta P_\parallel}{B_0}\right) \\ & + \frac{c\boldsymbol{b}_0\times\nabla B_0}{Z}\cdot\nabla\left(\frac{\delta P_\perp}{B_0^2}\right) + \frac{c\nabla\times\boldsymbol{b}_0\cdot\nabla B_0}{ZB_0^2}\delta P_\perp \\ & + \frac{c\nabla\times\boldsymbol{b}_0}{B_0}\cdot n_0\nabla\phi + \delta\boldsymbol{B}\cdot\nabla\left(\frac{n_0\delta u_\parallel}{B_0}\right) \\ & + B_0\boldsymbol{v}_E\cdot\nabla\left(\frac{\delta n}{B_0}\right) + \frac{c\,\delta n}{B_0^2}\boldsymbol{b}_0\times\nabla B_0\cdot\nabla\phi \\ & + \frac{c\,\delta n}{B_0^2}\nabla\times\boldsymbol{B}_0\cdot\nabla\phi, \end{aligned} \tag{20}$$

$$0 = \partial_t\,\delta n + \delta\boldsymbol{B}\cdot\nabla\left(\frac{n_0 u_{\parallel 0}}{B_0}\right) + \boldsymbol{B}_0\cdot\nabla\left(\frac{n_0\,\delta u_\parallel}{B_0}\right) + B_0\boldsymbol{v}_E\cdot\nabla\left(\frac{n_0}{B_0}\right) - n_0(\delta\boldsymbol{v}_* + \boldsymbol{v}_E)\cdot\frac{\nabla B_0}{B_0} + \frac{c\nabla\times\boldsymbol{B}_0}{ZB_0^2}\cdot\nabla\,\delta P_\parallel + \frac{c\nabla\times\boldsymbol{B}_0\cdot\nabla B_0}{ZB_0^3}(\delta P_\perp - \delta P_\parallel) + n_0\frac{c\nabla\times\boldsymbol{B}_0}{B_0^2}\cdot\nabla\phi + \delta\boldsymbol{B}\cdot\nabla\left(\frac{n_0\delta u_\parallel}{B_0}\right) + B_0\boldsymbol{v}_E\cdot\nabla\left(\frac{\delta n}{B_0}\right) + \frac{c\,\delta n}{B_0^2}\boldsymbol{b}_0\times\nabla B_0\cdot\nabla\phi + \frac{c\,\delta n}{B_0^2}\nabla\times\boldsymbol{B}_0\cdot\nabla\phi, \tag{21}$$

where

$$\delta n = \int_{\mathrm{GC}} \mathrm{d}\boldsymbol{v}\,\delta f, \tag{22}$$

$$\delta u_\parallel = \frac{1}{n_0}\int_{\mathrm{GC}} \mathrm{d}\boldsymbol{v} v_\parallel\,\delta f, \tag{23}$$

$$\delta P_\parallel = \int_{\mathrm{GC}} \mathrm{d}\boldsymbol{v} m v_\parallel^2\,\delta f, \tag{24}$$

$$\delta P_\perp = \int_{\mathrm{GC}} \mathrm{d}\boldsymbol{v}\mu B_0\,\delta f, \tag{25}$$

and

$$\delta\boldsymbol{v}_* = \frac{c}{n_0 Z B_0}\boldsymbol{b}_0\times\nabla(\delta P_\perp + \delta P_\parallel) \tag{26}$$

is the perturbed diamagnetic drift velocity. Apply (20) and (21) to the electrons ($Z_\mathrm{e} = -e$):

$$0 = \partial_t\,\delta n_\mathrm{e} + \delta\boldsymbol{B}\cdot\nabla\left(\frac{n_{0\mathrm{e}} u_{\parallel 0\mathrm{e}}}{B_0}\right) + B_0\boldsymbol{v}_E\cdot\nabla\left(\frac{n_{0\mathrm{e}}}{B_0}\right) + \boldsymbol{B}_0\cdot\nabla\left(\frac{n_{0\mathrm{e}}\,\delta u_{\parallel\mathrm{e}}}{B_0}\right) - \frac{c\nabla\times\boldsymbol{b}_0}{e}\cdot\nabla\left(\frac{\delta P_{\parallel\mathrm{e}}}{B_0}\right) - \frac{c\boldsymbol{b}_0\times\nabla B_0}{e}\cdot\nabla\left(\frac{\delta P_{\perp\mathrm{e}}}{B_0^2}\right) - \frac{c\nabla\times\boldsymbol{b}_0\cdot\nabla B_0}{eB_0^2}\,\delta P_{\perp\mathrm{e}} + \frac{c\nabla\times\boldsymbol{b}_0}{B_0}\cdot n_{0\mathrm{e}}\nabla\phi + \delta\boldsymbol{B}\cdot\nabla\left(\frac{n_{0\mathrm{e}}\delta u_{\parallel\mathrm{e}}}{B_0}\right) + B_0\boldsymbol{v}_E\cdot\nabla\left(\frac{\delta n_\mathrm{e}}{B_0}\right) + \frac{c\,\delta n_\mathrm{e}}{B_0^2}\boldsymbol{b}_0\times\nabla B_0\cdot\nabla\phi + \frac{c\,\delta n_\mathrm{e}}{B_0^2}\nabla\times\boldsymbol{B}_0\cdot\nabla\phi, \tag{27}$$

$$0 = \partial_t\,\delta n_\mathrm{e} + \boldsymbol{B}_0\cdot\nabla\left(\frac{n_{0\mathrm{e}}\,\delta u_{\parallel\mathrm{e}}}{B_0}\right) + B_0\boldsymbol{v}_E\cdot\nabla\left(\frac{n_{0\mathrm{e}}}{B_0}\right) - n_{0\mathrm{e}}(\delta\boldsymbol{v}_{*\mathrm{e}} + \boldsymbol{v}_E)\cdot\frac{\nabla B_0}{B_0} + \delta\boldsymbol{B}\cdot\nabla\left(\frac{n_{0\mathrm{e}}u_{\parallel 0\mathrm{e}}}{B_0}\right) + \frac{c\nabla\times\boldsymbol{B}_0}{B_0^2}\cdot\left[-\frac{\nabla\delta P_{\parallel\mathrm{e}}}{e} - \frac{(\delta P_{\perp\mathrm{e}} - \delta P_{\parallel\mathrm{e}})\nabla B_0}{eB_0} + n_{0\mathrm{e}}\nabla\phi\right] + \delta\boldsymbol{B}\cdot\nabla\left(\frac{n_{0\mathrm{e}}\delta u_{\parallel\mathrm{e}}}{B_0}\right) + B_0\boldsymbol{v}_E\cdot\nabla\left(\frac{\delta n_\mathrm{e}}{B_0}\right) + \frac{c\,\delta n_\mathrm{e}}{B_0^2}\boldsymbol{b}_0\times\nabla B_0\cdot\nabla\phi + \frac{c\,\delta n_\mathrm{e}}{B_0^2}\nabla\times\boldsymbol{B}_0\cdot\nabla\phi. \tag{28}$$

The first four terms in (28) are identical to the electron continuity equation (10) in [1]. The fifth and the sixth terms are introduced by the parallel equilibrium flow $u_{\parallel 0\mathrm{e}}$ and finite $\nabla\times\boldsymbol{B}_0$. The last four terms are nonlinear terms. The parallel equilibrium flow and current terms are verified in RSAE simulations shown in section 4. The nonlinear terms will be verified in future nonlinear Alfvén eigenmode simulations.

2.2. Particle weight evolution equations

We assume that the equilibrium distribution is a shifted Maxwellian for all particle species:

$$f_{0\alpha} = \frac{n_{0\alpha}}{(2\pi v_{\mathrm{th},\alpha}^2)^{3/2}}\exp\left[\frac{-(v_\parallel - u_{\parallel 0\alpha})^2 - \frac{2\mu B_0}{m_\alpha}}{2v_{\mathrm{th},\alpha}^2}\right] \qquad \alpha = \mathrm{i},\,\mathrm{e}, \tag{29}$$

where $u_{\parallel 0\alpha}$ is the parallel equilibrium flow velocity, and $v_{\mathrm{th},\alpha} = \sqrt{T_\alpha/m_\alpha}$ is the thermal velocity. The weight evolution equation for ions reads [1]:

$$\frac{\mathrm{d}w_\mathrm{i}}{\mathrm{d}t} = (1-w_\mathrm{i})\left\{-\left(v_\parallel\frac{\delta\boldsymbol{B}}{B_0} + \boldsymbol{v}_E\right)\cdot\boldsymbol{\kappa}_\mathrm{i} + \frac{u_{\parallel 0\mathrm{i}}\mu}{T_\mathrm{i}}\frac{\delta\boldsymbol{B}}{B_0}\cdot\nabla B_0 - \frac{Z_\mathrm{i}}{T_\mathrm{i}}(v_\parallel - u_{\parallel 0\mathrm{i}})\left(\boldsymbol{b}_0\cdot\nabla\phi + \frac{1}{c}\partial_t A_\parallel\right) - \frac{Z_\mathrm{i}}{T_\mathrm{i}}\left[\boldsymbol{v}_\mathrm{g} + \left(1 - \frac{u_{\parallel 0\mathrm{i}}}{v_\parallel}\right)\boldsymbol{v}_\mathrm{c}\right]\cdot\nabla\phi\right\}. \tag{30}$$

The weight evolution equation for electrons reads [1]

$$\frac{\mathrm{d}w_\mathrm{e}}{\mathrm{d}t} = \left(1 + \frac{\delta f_\mathrm{e}^{(0)}}{f_{0\mathrm{e}}} + w_\mathrm{e}\right)\left\{-\boldsymbol{v}_\mathrm{E}\cdot\boldsymbol{\kappa}_\mathrm{e} - \partial_t\frac{\delta f_\mathrm{e}^{(0)}}{f_{0\mathrm{e}}} - (\boldsymbol{v}_\mathrm{g} + \boldsymbol{v}_\mathrm{c})\cdot\nabla\frac{\delta f_\mathrm{e}^{(0)}}{f_{0\mathrm{e}}} + \frac{e}{T_\mathrm{e}}\left[\boldsymbol{v}_\mathrm{g} + \boldsymbol{v}_\mathrm{c}\left(1 - \frac{u_{\parallel 0\mathrm{e}}}{v_\parallel}\right)\right]\cdot\nabla\phi - \frac{c\boldsymbol{b}_0\times\nabla\phi_{00}}{B_0}\cdot\nabla\frac{\delta f_\mathrm{e}^{(0)}}{f_{0\mathrm{e}}} + (v_\parallel - u_{\parallel 0\mathrm{e}})\frac{e}{cT_\mathrm{e}}\partial_t A_{\parallel 00} - \frac{e}{T_\mathrm{e}}u_{\parallel 0\mathrm{e}}\,\delta E_\parallel + u_{\parallel 0\mathrm{e}}\frac{\mu}{T_\mathrm{e}}\frac{\delta\boldsymbol{B}}{B_0}\cdot\nabla B_0\right\}, \tag{31}$$

where $\delta f_\mathrm{e}^{(0)}$ is the adiabatic component of the electron perturbed distribution function, $\delta E_\parallel$ is the nonzonal component of the parallel electric field. In (30) and (31), $\boldsymbol{\kappa}_\alpha$ is given by

$$\boldsymbol{\kappa}_\alpha = \frac{\nabla n_{0\alpha}}{n_{0\alpha}} + \left[\frac{\mu B_0}{T_\alpha} + \frac{m_\alpha(v_\parallel - u_{\parallel 0\alpha})^2}{2T_\alpha} - \frac{3}{2}\right]\frac{\nabla T_\alpha}{T_\alpha} + \frac{m(v_\parallel - u_{\parallel 0\alpha})\nabla u_{\parallel 0\alpha}}{T_\alpha}. \tag{32}$$

The curvature drift operator in (30) and (31) reads

$$\boldsymbol{v}_\mathrm{c}\cdot\nabla = \frac{m_\alpha c v_\parallel^2}{Z_\alpha B_0^3}\boldsymbol{B}_0\times\nabla B_0\cdot\nabla + \frac{m_\alpha c v_\parallel^2}{Z_\alpha B_0^2}\nabla\times\boldsymbol{B}_0\cdot\nabla. \tag{33}$$

In previous implementation, the second term on the right-hand side in (33) is dropped because it is on the order of $k_\parallel/k_\perp$ compared with the first term. Here this term is retained for consistency as all the $\nabla\times\boldsymbol{B}_0$ terms are retained in this formulation. Also implemented is the parallel Ampère law

$$Z_\mathrm{i}n_{0\mathrm{i}}u_{\parallel 0\mathrm{i}} - en_{0\mathrm{e}}u_{\parallel 0\mathrm{e}} = \frac{c}{4\pi}\boldsymbol{b}_0\cdot\nabla\times\boldsymbol{B}_0 \tag{34}$$

being enforced on the equilibrium flows of all species for a given $\boldsymbol{B}_0$ from equilibrium solver such as EFIT.

3. Reduction of gyrokinetic formulation to linear ideal MHD

In this section, we prove that in the linear and long wavelength limit, the gyrokinetic formulation described in section 2 reduces to the ideal MHD eigenmode equation (A.9) in appendix A.

3.1. Reduction of gyrokinetic Poisson's equation and Ampère's law

The integral $\int_{\boldsymbol{X}\to\boldsymbol{x}} \mathrm{d}\boldsymbol{v}$ in (8) has two parts as can be seen in (11). The first part, which is over the gyro-centre velocity space, is the same as $\int_{\mathrm{GC}} \mathrm{d}\boldsymbol{v}$ defined in (14). The second part of the integral, which is the transformation between the gyro-centre coordinates and the particle coordinates, gives rise to an operator $\mathfrak{J}_0(k_\perp\rho)$, where $\mathfrak{J}_0()$ is the Bessel function. In GTC, this $\mathfrak{J}_0(k_\perp\rho)$ is implemented accurately in the charge scattering from each particle's gyro-centre to its gyro-orbit when collecting charges from the particles [9]. Note that the gyro-averaging on the perturbed field quantities also gives rise to an operator $\mathfrak{J}_0(k_\perp\rho)$ [13]:

$$\langle\delta\phi\rangle_{\mathrm{c}} = \mathfrak{J}_0(k_\perp\rho)\,\delta\phi. \tag{35}$$

In the long wavelength limit of $k_\perp\rho_{\mathrm{i}} < 1$, for comparison with ideal MHD theory, we can expand the $\mathfrak{J}_0^2$ operator and keep terms up to $O(k_\perp^2\rho^2)$:

$$\begin{aligned}\mathfrak{J}_0^2(k_\perp\rho_{\mathrm{i}}) &= \mathfrak{J}_0^2\left(k_\perp\frac{\sqrt{2\mu B_0/m_{\mathrm{i}}}}{\Omega_{\mathrm{i}}}\right)\\ &\approx 1-\frac{\mu m_{\mathrm{i}}c^2}{Z_{\mathrm{i}}^2B_0}k_\perp^2\\ &= 1+\frac{\mu m_{\mathrm{i}}c^2}{Z_{\mathrm{i}}^2B_0}\nabla_\perp^2.\end{aligned} \tag{36}$$

Then $\delta\tilde{\phi}_{\mathrm{i}}$ becomes [9]

$$\delta\tilde{\phi} \approx \delta\phi + \frac{m_{\mathrm{i}}c^2T_{\mathrm{i}}}{Z_{\mathrm{i}}^2B_0^2}\nabla_\perp^2\,\delta\phi. \tag{37}$$

Equation (6) reduces to

$$\begin{aligned}\sum_{\alpha=\mathrm{i,e}} Z_\alpha\,\delta n_\alpha &= \frac{Z_{\mathrm{i}}^2n_{\mathrm{i}}}{T_{\mathrm{i}}}(\delta\phi-\delta\tilde{\phi})\\ &\approx -\frac{n_{0\mathrm{i}}m_{\mathrm{i}}c^2}{B_0^2}\nabla_\perp^2\,\delta\phi\\ &= -\frac{c^2}{4\pi v_{\mathrm{A}}^2}\nabla_\perp^2\,\delta\phi,\end{aligned} \tag{38}$$

where

$$v_{\mathrm{A}}^2 = \frac{B_0^2}{4\pi n_{0\mathrm{i}}m_{\mathrm{i}}}. \tag{39}$$

In the ideal MHD limit, the parallel electric field is zero, $\delta E_\parallel = 0$, and as a result:

$$\partial_t\,\delta A_\parallel = -c\boldsymbol{b}_0\cdot\nabla\,\delta\phi. \tag{40}$$

We combine (38), (7) and (40), and take the linear normal mode theory substitutions $\partial_t \to -\mathrm{i}\omega$ and $\boldsymbol{b}_0\cdot\nabla \to \mathrm{i}k_\parallel$ to get a reduced equation:

$$\begin{aligned}&\frac{\omega^2}{v_{\mathrm{A}}^2}\nabla_\perp^2\,\delta\phi + \mathrm{i}\boldsymbol{B}_0\cdot\nabla\left[\frac{\nabla_\perp^2(k_\parallel\,\delta\phi)}{B_0}\right]\\ &\quad+\mathrm{i}\omega\frac{4\pi}{c^2}\sum_\alpha(-\mathrm{i}\omega Z_\alpha\,\delta n_\alpha+\nabla\cdot\delta\boldsymbol{J}_{\parallel\alpha}) = 0.\end{aligned} \tag{41}$$

3.2. Reduction of ion gyrokinetic equation

To obtain an equation describing δn_{i} and $\delta J_{\parallel\mathrm{i}}$ for the ion species, we operate $\int_{\boldsymbol{X}\to\boldsymbol{x}}\mathrm{d}\boldsymbol{v}$ on the gyrokinetic equation (1). Similar to (35), the gyro-averaging gives rise to a $\mathfrak{J}_0(k_\perp\rho_{\mathrm{i}})$ operator:

$$\langle\delta\boldsymbol{B}\rangle_{\mathrm{c}} = \mathfrak{J}_0(k_\perp\rho_{\mathrm{i}})\,\delta\boldsymbol{B}, \tag{42}$$

$$\langle A_\parallel\rangle_{\mathrm{c}} = \mathfrak{J}_0(k_\perp\rho_{\mathrm{i}})A_\parallel. \tag{43}$$

We integrate the gyrokinetic equation in the linear limit,

$$\begin{aligned}0 &= \int_{\boldsymbol{X}\to\boldsymbol{x}}\mathrm{d}\boldsymbol{v}(\partial_t+\dot{\boldsymbol{X}}\cdot\nabla+\dot{v}_\parallel\partial_{v_\parallel})(f_{0\mathrm{i}}+\delta f_{\mathrm{i}})\\ &= \boldsymbol{B}_0\cdot\nabla\left(\frac{n_{0\mathrm{i}}u_{\parallel0\mathrm{i}}}{B_0}\right)+\frac{c\nabla\times\boldsymbol{b}_0}{Z_{\mathrm{i}}}\cdot\nabla\left(\frac{P_{\parallel0\mathrm{i}}}{B_0}\right)\\ &\quad+\frac{c\boldsymbol{b}_0\times\nabla B_0}{Z_{\mathrm{i}}}\cdot\nabla\left(\frac{P_{\perp0\mathrm{i}}}{B_0^2}\right)+\frac{c\nabla\times\boldsymbol{b}_0\cdot\nabla B_0}{Z_{\mathrm{i}}B_0^2}P_{\perp0\mathrm{i}}\\ &\quad+\partial_t\,\delta n_{\mathrm{i}}+\delta\boldsymbol{B}\cdot\nabla\left(\frac{n_{0\mathrm{i}}u_{\parallel0\mathrm{i}}}{B_0}\right)+B_0\boldsymbol{v}_E\cdot\nabla\left(\frac{n_{0\mathrm{i}}}{B_0}\right)\\ &\quad+\boldsymbol{B}_0\cdot\nabla\left(\frac{n_{0\mathrm{i}}\,\delta u_{\parallel\mathrm{i}}}{B_0}\right)+\frac{c\nabla\times\boldsymbol{b}_0}{Z_{\mathrm{i}}}\cdot\nabla\left(\frac{\delta P_{\parallel\mathrm{i}}}{B_0}\right)\\ &\quad+\frac{c\boldsymbol{b}_0\times\nabla B_0}{Z_{\mathrm{i}}}\cdot\nabla\left(\frac{\delta P_{\perp\mathrm{i}}}{B_0^2}\right)+\frac{c\nabla\times\boldsymbol{b}_0\cdot\nabla B_0}{Z_{\mathrm{i}}B_0^2}\,\delta P_{\perp\mathrm{i}}\\ &\quad+\frac{c\nabla\times\boldsymbol{b}_0}{B_0}\cdot n_{0\mathrm{i}}\nabla\,\delta\phi+\frac{m_{\mathrm{i}}c^2}{Z_{\mathrm{i}}^2B_0}(\nabla_\perp^2\,\delta\boldsymbol{B})\cdot\nabla\left(\frac{P_{0\mathrm{i}}u_{\parallel0\mathrm{i}}}{B_0^2}\right)\\ &\quad-\frac{m_{\mathrm{i}}c^3\boldsymbol{b}_0\times\nabla P_{0\mathrm{i}}}{Z_{\mathrm{i}}^2B_0^2}\cdot\nabla\frac{\nabla_\perp^2\,\delta\phi}{B_0}\\ &\quad+\frac{m_{\mathrm{i}}c^3P_{0\mathrm{i}}(3\boldsymbol{b}_0\times\nabla B_0+\nabla\times\boldsymbol{B}_0)}{Z_{\mathrm{i}}^2B_0^3}\cdot\nabla\frac{\nabla_\perp^2\,\delta\phi}{B_0}.\end{aligned} \tag{44}$$

This equation can be separated into the equilibrium continuity equation:

$$\begin{aligned}&\boldsymbol{B}_0\cdot\nabla\left(\frac{n_{0\mathrm{i}}u_{\parallel0\mathrm{i}}}{B_0}\right)+\frac{c\nabla\times\boldsymbol{b}_0}{Z_{\mathrm{i}}}\cdot\nabla\left(\frac{P_{\parallel0\mathrm{i}}}{B_0}\right)\\ &\quad+\frac{c\boldsymbol{b}_0\times\nabla B_0}{Z_{\mathrm{i}}}\cdot\nabla\left(\frac{P_{\perp0\mathrm{i}}}{B_0^2}\right)+\frac{c\nabla\times\boldsymbol{b}_0\cdot\nabla B_0}{Z_{\mathrm{i}}B_0^2}P_{\perp0\mathrm{i}} = 0,\end{aligned} \tag{45}$$

and the linear continuity equation:

$$\begin{aligned}0 &= \partial_t\,\delta n_{\mathrm{i}}+\delta\boldsymbol{B}\cdot\nabla\left(\frac{n_{0\mathrm{i}}u_{\parallel0\mathrm{i}}}{B_0}\right)+B_0\boldsymbol{v}_E\cdot\nabla\left(\frac{n_{0\mathrm{i}}}{B_0}\right)\\ &\quad+\boldsymbol{B}_0\cdot\nabla\left(\frac{n_{0\mathrm{i}}\,\delta u_{\parallel\mathrm{i}}}{B_0}\right)+\frac{c\nabla\times\boldsymbol{b}_0}{Z_{\mathrm{i}}}\cdot\nabla\left(\frac{\delta P_{\parallel\mathrm{i}}}{B_0}\right)\\ &\quad+\frac{c\boldsymbol{b}_0\times\nabla B_0}{Z_{\mathrm{i}}}\cdot\nabla\left(\frac{\delta P_{\perp\mathrm{i}}}{B_0^2}\right)+\frac{c\nabla\times\boldsymbol{b}_0\cdot\nabla B_0}{Z_{\mathrm{i}}B_0^2}\,\delta P_{\perp\mathrm{i}}\\ &\quad+\frac{c\nabla\times\boldsymbol{b}_0}{B_0}\cdot n_{0\mathrm{i}}\nabla\,\delta\phi+\underbrace{\frac{m_{\mathrm{i}}c^2}{Z_{\mathrm{i}}^2B_0}(\nabla_\perp^2\,\delta\boldsymbol{B})\cdot\nabla\left(\frac{P_{0\mathrm{i}}u_{\parallel0\mathrm{i}}}{B_0^2}\right)}_{\{\mathrm{i}\}}\end{aligned}$$

$$\underbrace{-\frac{m_i c^3 \boldsymbol{b}_0 \times \nabla P_{0i}}{Z_i^2 B_0^2} \cdot \nabla \frac{\nabla_\perp^2 \delta\phi}{B_0}}_{\{ii\}}$$
$$\underbrace{+\frac{m_i c^3 P_{0i}(3\boldsymbol{b}_0 \times \nabla B_0 + \nabla \times \boldsymbol{B}_0)}{Z_i^2 B_0^3} \cdot \nabla \frac{\nabla_\perp^2 \delta\phi}{B_0}}_{\{iii\}}. \quad (46)$$

These two equations are the same as those of the electrons (15) and (20) in the linear limit except for the last three terms in (46), which are introduced by the ion finite Larmor radius (FLR) effects. In the $k_\perp L_{B_0} \sim k_\perp R_0 \gg 1$ limit (but still $k_\perp \rho_i \ll 1$), the term {ii} becomes:

$$\{ii\} \approx -\frac{m_i c^2 n_{0i}}{Z_i B_0^2} \frac{c\boldsymbol{b}_0 \times \nabla P_{0i}}{Z_i B_0 n_{0i}} \cdot \nabla \nabla_\perp^2 \delta\phi$$
$$= -\frac{m_i c^2 n_{0i}}{Z_i B_0^2} \boldsymbol{v}_{*i} \cdot \nabla \nabla_\perp^2 \delta\phi, \quad (47)$$

where

$$\boldsymbol{v}_{*i} = \frac{c\boldsymbol{b}_0 \times \nabla P_{0i}}{Z_i B_0 n_{0i}}. \quad (48)$$

This term is responsible for producing the kinetic ballooning mode [14]. We compare the ordering of this term with the other two FLR terms:

$$O\left(\frac{\{iii\}}{\{ii\}}\right) \sim \frac{L_{P_{0i}}}{L_{B_0}}, \quad (49)$$

$$O\left(\frac{\{i\}}{\{ii\}}\right) \sim \frac{k_\parallel u_{\parallel 0i}}{\omega}\left(1 + \frac{L_{P_{0i}}}{L_{u_{\parallel 0i}}} - 2\frac{L_{P_{0i}}}{L_{B_0}}\right), \quad (50)$$

where $L_{(\cdot)} \equiv 1/|\nabla \ln(\cdot)|$ denotes the characteristic gradient length. In the case of $L_{P_{0i}} < L_{B_0}, L_{P_{0i}} \lesssim L_{u_{\parallel 0i}}$ and $k_\parallel u_{\parallel 0i} \ll \omega$, the terms {i} and {iii} are not important and can be dropped. For typical tokamak scalings, $L_{B_0} \sim R_0$, $L_{P_{0i}} \sim a$, $L_{u_{\parallel 0i}} \gtrsim a$ and $u_{\parallel 0i} \ll v_A \sim \omega/k_\parallel$, so $L_{P_{0i}} < L_{B_0}$, $L_{P_{0i}} \lesssim L_{u_{\parallel 0i}}$ and $k_\parallel u_{\parallel 0i} \ll \omega$ are usually satisfied. Keeping term {ii} as the only FLR effect, the ion continuity equation becomes

$$Z_i \partial_t \delta n_i + \boldsymbol{B}_0 \cdot \nabla\left(\frac{Z_i n_{0i} \delta u_{\parallel i}}{B_0}\right) = -i\omega Z_i \delta n_i + \nabla \cdot \delta \boldsymbol{J}_{\parallel i}$$
$$\approx -\delta \boldsymbol{B} \cdot \nabla\left(\frac{J_{\parallel 0i}}{B_0}\right) - B_0 \boldsymbol{v}_E \cdot \nabla\left(\frac{Z_i n_{0i}}{B_0}\right)$$
$$+ \frac{m_i c^2 n_{0i}}{B_0^2} \boldsymbol{v}_{*i} \cdot \nabla \nabla_\perp^2 \delta\phi - c\nabla \times \boldsymbol{b}_0 \cdot \nabla\left(\frac{\delta P_{\parallel i}}{B_0}\right)$$
$$- c\boldsymbol{b}_0 \times \nabla B_0 \cdot \nabla\left(\frac{\delta P_{\perp i}}{B_0^2}\right) - \frac{c\nabla \times \boldsymbol{b}_0 \cdot \nabla B_0}{B_0^2} \delta P_{\perp i}$$
$$- \frac{c\nabla \times \boldsymbol{b}_0}{B_0} \cdot Z_i n_{0i} \nabla \delta\phi. \quad (51)$$

3.3. Reduction to linear ideal MHD

The electron continuity equation (27) in the linear limit is

$$-e\partial_t \delta n_e - \boldsymbol{B}_0 \cdot \nabla\left(\frac{e n_{0e} \delta u_{\parallel e}}{B_0}\right) = i\omega e \delta n_e + \nabla \cdot \delta \boldsymbol{J}_{\parallel e}$$
$$= -\delta \boldsymbol{B} \cdot \nabla\left(\frac{J_{\parallel 0e}}{B_0}\right) + B_0 \boldsymbol{v}_E \cdot \nabla\left(\frac{e n_{0e}}{B_0}\right)$$
$$- c\nabla \times \boldsymbol{b}_0 \cdot \nabla\left(\frac{\delta P_{\parallel e}}{B_0}\right) - c\boldsymbol{b}_0 \times \nabla B_0 \cdot \nabla\left(\frac{\delta P_{\perp e}}{B_0^2}\right)$$
$$- \frac{c\nabla \times \boldsymbol{b}_0 \cdot \nabla B_0}{B_0^2} \delta P_{\perp e} + \frac{c\nabla \times \boldsymbol{b}_0}{B_0} \cdot e n_{0e} \nabla \delta\phi. \quad (52)$$

Plugging (52) and (51) into (41), and considering (39), quasi-neutrality $\sum_\alpha Z_\alpha n_{0\alpha} = 0$ and Ampère's law for equilibrium $\sum_\alpha J_{\parallel 0\alpha} = \frac{c}{4\pi} \boldsymbol{b}_0 \cdot \nabla \times \boldsymbol{B}_0$, we obtain:

$$0 = \frac{\omega(\omega - \omega_{*P})}{v_A^2} \nabla_\perp^2 \delta\phi + i\boldsymbol{B}_0 \cdot \nabla\left[\frac{\nabla_\perp^2 (k_\parallel \delta\phi)}{B_0}\right]$$
$$- i\nabla(k_\parallel \delta\phi) \times \boldsymbol{b}_0 \cdot \nabla\left(\frac{\boldsymbol{b}_0 \cdot \nabla \times \boldsymbol{B}_0}{B_0}\right)$$
$$- i\omega \frac{4\pi}{c}\left[\nabla \times \boldsymbol{b}_0 \cdot \nabla\left(\frac{\delta P_\parallel}{B_0}\right) + \boldsymbol{b}_0 \times \nabla B_0 \cdot \nabla\left(\frac{\delta P_\perp}{B_0^2}\right)\right.$$
$$\left. + \frac{\nabla \times \boldsymbol{b}_0 \cdot \nabla B_0}{B_0^2} \delta P_\perp\right], \quad (53)$$

where $\delta P_\parallel = \sum_\alpha \delta P_{\parallel\alpha}$, $\delta P_\perp = \sum_\alpha \delta P_{\perp\alpha}$, and

$$\omega_{*P} = -i\boldsymbol{v}_{*i} \cdot \nabla \quad (54)$$

is the ion diamagnetic frequency. Note that ω_{*P} only operates on perturbed quantities.

Now the first three terms of (53) match those of the ideal MHD eigenmode equation (A.9) in appendix A. The last term of (53), i.e. the pressure term, looks different from the corresponding term of (A.9). In appendices B and C, we show that the difference is negligible. Therefore, the gyrokinetic formulation reduces to the ideal MHD theory in the linear and long wavelength limit.

The first term in (53) is the inertial term, with the ω_{*P} term responsible for the kinetic ballooning mode. The second term is the field line bending term responsible for the shear Alfvén wave. The third term is the current driving term. Most previous gyrokinetic simulations drop this current driving term. Retaining this term in this formulation gives the capability to simulate current-driven modes such as the kink mode. The last term is the pressure gradient term responsible for pressure-driven instabilities such as the interchange instability and the ideal ballooning mode. Equation (53) shows that gyrokinetic simulation can be used to study kinetic MHD modes including interchange modes, kink modes and shear Alfvén waves excited by energetic particles, where kinetic effects are important.

4. Parallel equilibrium current effects on RSAE

The gyrokinetic simulation model with equilibrium current and nonlinear terms has been implemented in GTC. The implementation details are given in appendices D and E. In this section, we verify the simulation model by demonstrating the effects of equilibrium current on RSAE as predicted by theory.

4.1. Analytic calculation

In a reversed shear tokamak with concentric-circular flux surfaces, in a uniform plasma and zero-β limit, (53) for one n and m harmonic $\delta\phi(r, \theta, \zeta) = \delta\hat{\phi}(r) \exp[i(n\zeta - m\theta)]$ near the $q_{\min}$ surface becomes [4]

$$\frac{1}{r}\frac{d}{dr}\left(r\Lambda \frac{d}{dr}\delta\hat{\phi}\right) - \frac{m^2}{r^2}\Lambda \delta\hat{\phi} - \frac{D}{r}\delta\hat{\phi} = 0, \quad (55)$$

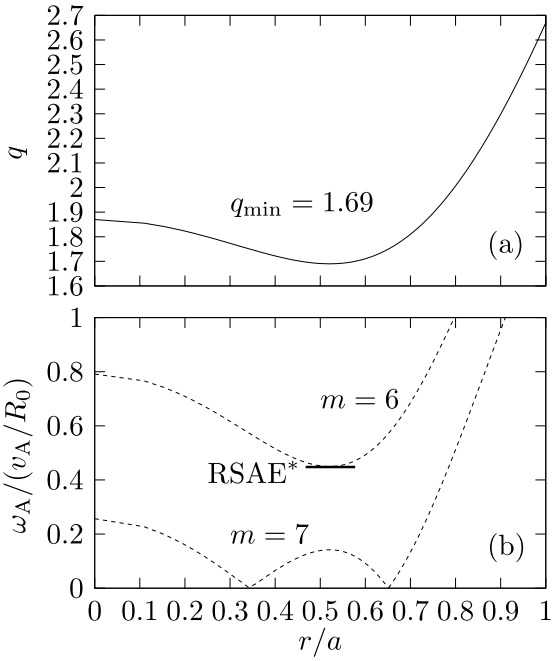

Figure 1. (*a*) Safety factor q-profile. (*b*) Alfvén continua of $n = 4, m = 6$ and $n = 4, m = 7$ in the ideal MHD limit and without linear toroidal coupling; RSAE*: frequency of $m = 6$ RSAE without equilibrium current (0.448 v_{A0}/R_0).

where

$$\Lambda = \frac{\omega^2}{v_A^2} - k_\parallel^2, \tag{56}$$

and D represents contributions from fast ion pressure [6], background plasma pressure gradient [15], toroidal coupling [16], magnetic shear, etc. The first two terms of (55) give the Alfvén continuum. The last term determines whether an eigenmode exists near the Alfvén continuum extremum. Here we only consider the magnetic shear effect to examine the effects of the parallel equilibrium current $\boldsymbol{b}_0 \cdot \nabla \times \boldsymbol{B}_0$. When the parallel equilibrium current is ignored,

$$D = k_\parallel k_\parallel' + r k_\parallel k_\parallel''. \tag{57}$$

The prime symbol ($'$) in this section denotes the derivative with respect to r. At the $q_{\min}$ surface, noting that $k_\parallel' = 0$ and $k_\parallel'' \neq 0$, D is nonzero and an RSAE exists as can be shown by numerically solving (55). With the inclusion of parallel equilibrium current [6],

$$D = -2 k_\parallel k_\parallel', \tag{58}$$

which is zero at the $q_{\min}$ surface and thus eigenmode does not exist. Note that other effects contributing to D mentioned above can also form an eigenmode.

4.2. Verification in simulation

To verify the implementation of the equilibrium current, we simulate a tokamak case with concentric-circular flux surfaces. The parameters are taken from [4]. The q-profile is shown in figure 1(*a*), whose corresponding Alfvén continua of $n = 4, m = 6$ and $n = 4, m = 7$ without linear toroidal coupling are shown in figure 1(*b*). The $n = 4, m = 6$ mode is studied here to avoid complication by the toroidal coupling effect, because the toroidal coupling effect cannot make an RSAE below the continuum minimum [16]. In the ideal MHD limit, RSAE exists when the equilibrium current is not taken into account.

The differences between the simulations without and with the equilibrium current can be seen in the contour plots of $\delta\phi$ in the radial-time space in figure 2. Figure 2(*a*) corresponds to the case without the equilibrium current. An eigenmode exists and the mode structures are horizontal, indicating that $\delta\phi$ at different radial locations oscillates at the same eigenmode frequency. For the case with the equilibrium current shown in figure 2(*b*), where no eigenmode exists, $\delta\phi$ at every radial location oscillates at the local continuum frequency, leading to the bending of the mode structures or the so-called phase mixing. The fast damping of the mode amplitude due to the phase mixing in figure 2(*b*) also indicates that there is no eigenmode in this case. Therefore, the simulation results are consistent with the analytic calculation in section 4.1.

5. Conclusion

A nonlinear gyrokinetic simulation model incorporating equilibrium current has been formulated for studying kinetic magnetohydrodynamic processes in magnetized plasmas. This complete formulation enables gyrokinetic simulation of both pressure-gradient-driven and current-driven instabilities as well as their nonlinear interactions in multi-scale simulations. The gyrokinetic simulation model recovers the ideal magnetohydrodynamic theory in the linear long wavelength regime including ideal and kinetic ballooning modes, kink modes and shear Alfvén waves. The implementation of this model in the global gyrokinetic particle code has been verified for the simulation of the effects of equilibrium current on the reversed shear Alfvén eigenmode in tokamaks.

Acknowledgments

The authors acknowledge useful discussions with L. Chen, P. Porazik, Z. Wang, Y. Xiao and H. Zhang. This work was supported by the US Department of Energy (DOE) SciDAC GSEP center and, in part, by the NSF. Simulations were performed using supercomputers at NERSC and ORNL.

Appendix A. Linear ideal MHD theory with equilibrium current

We begin with the single-fluid linearized momentum equation of the ideal MHD theory [17].

$$n_{0i} m_i (\partial_t + \boldsymbol{v}_0 \cdot \nabla) \delta\boldsymbol{v} + \nabla \cdot \delta\mathbb{P} = \frac{1}{c} (\delta\boldsymbol{J}_\perp \times \boldsymbol{B}_0 + \boldsymbol{J}_0 \times \delta\boldsymbol{B}), \tag{A.1}$$

where the leading order of the equilibrium velocity is the ion diamagnetic velocity:

$$\boldsymbol{v}_0 = \boldsymbol{v}_*, \tag{A.2}$$

with $\boldsymbol{v}_{*i}$ defined in (48). The leading order of the perturbed velocity is the $\boldsymbol{E} \times \boldsymbol{B}$ drift:

$$\delta\boldsymbol{v}_\perp = \frac{c\boldsymbol{b}_0 \times \nabla\, \delta\phi}{B_0}. \tag{A.3}$$